DEVELOPMENT OF A HIGHLY INTEGRATED LASER DRIVER WITH A NIR DISTRIBUTED FEEDBACK LASER FOR CO-SENSING SYSTEM

Bin LI[1], Yuqi ZHANG[2], Yaodan CHI[3], Xiaotian YANG[4], Yiding WANG[5]

A distributed feedback laser driving instrument was designed and developed specifically for a laser at 1563.06 nm which is applied for CO detection. This instrument can be applied as the integrated light source to meet the requirements of CO-sensing experiments based on wavelength modulation spectroscopy technique. It replaces commercial instruments including laser temperature controller, current driver and signal generator by using the self-developed circuit boards that are integrated inside the instrument. Experimental results demonstrate that the center wavelength can be effectively modulated by using the developed instrument suggesting good performance of the developed laser driver.

Keywords: near infrared (NIR), Distributed feedback laser; temperature control; spectroscopy measurement; CO detection

1. Introduction

Carbon monoxide (CO) is well-known as a hazard to mining safety because it is a common kind of toxic gases. It is also crucial to detect CO concentration in mining workplaces to prevent serf-combustion of coal. Compared with traditional gas-sensing techniques such as catalyst combustion [1-3], electrochemical [4-6] and semiconductor [7, 8], infrared absorption spectroscopy is widely researched due to numerous advantages including fast response, non-intrusive nature and sensitive species-specific detection capabilities [9-12]. Therefore, CO sensing systems and sensors based on infrared absorption spectroscopy have been reported by many research groups in recent years and

[1] Ph.D., Dept.of Electrical and Computer Engineering, Jilin Jianzhu University, China, e-mail: libin@jlju.edu.cn
[2] Stud., Dept.of Electrical and Computer Engineering, Jilin Jianzhu University, China, e-mail: 841753097@qq.com
[3] Prof., Dept.of Electrical and Computer Engineering, Jilin Jianzhu University, China, e-mail: 2484670561@qq.com
[4] Prof., Jilin Provincial Key Laboratory of Architectural Electricity & Comprehensive Energy Saving, Jilin Jianzhu University, China, e-mail: 870731919@qq.com
[5] Prof., State Key Laboratory on Integrated Optoelectronics, College of Electronic Science and Engineering, Jilin University, China, e-mail: wangyiding48@hotmail.com

many related techniques have been developed and improved to achieve high-sensitive sensing ability.

Wavelength Modulation Spectroscopy (WMS) technique is widely adopted in the trace gas detection field due to its capability of high-accuracy detection [13-16]. In WMS, lasers with center wavelength in the near infrared and middle infrared region are broadly applied as light sources. Emitting center wavelength sweeps across one absorption line of gas molecule periodically at a low frequency. Meanwhile, the laser is also modulated by a relative high frequency signal for the extraction of harmonic signals [17, 18]. In this way, experiments based on WMS are commonly utilizing commercial instruments including laser current driver and signal generator to satisfy the experimental requirements. Besides, laser diode temperature controller is also a type of essential instrument for accuracy experiments. By utilizing the commercial instruments mentioned above, lasers can be controlled effectively to meet the requirements of gas-sensing experiments based on infrared absorption spectroscopy techniques [19]. However, there are still some drawbacks of using the commercial instruments such as high expense, large size and difficult to integrate. These drawbacks are practical barriers for industrialization of WMS-based gas sensing technique and these problems should be solved.

In this paper, a cost-effective DFB laser driver was developed experimentally demonstrated. This laser driver is made of self-developed circuits and is integrated as a standalone instrument. It has the capability of controlling laser temperature, driving current and modulating essential signals based on the WMS technique. This instrument can be applied as the radiation source of CO detection system. The applied gas sensing theory is briefly discussed only to guide the audience and define units. Then, details of the key modules developed in this paper is demonstrated with individual tests. Finally, the spectroscopy is measured by using the self-developed instrument and results are discussed in the end of this paper.

2. Theoretic perspective

Wavelength modulation spectroscopy technique is widely applied word widely for its low-noise and high signal-noise radio feature. The foundations of laser absorption with WMS-2f detection requires controllable radiation source for generating desired spectrum containing modulation signal. Therefore, a brief summary of the laser driving theory related to WMS-2f detection is shown below before the demonstration of system details. According to the law of Lambert-Beer, $I(\upsilon)$ and $I_0(\upsilon)$ are emitting optical power and original optical power respectively shown in Eq. (1) below, where the frequency is expressed as υ and $\alpha(\upsilon,t)$ is the absorption coefficient. The concentration of gas is expressed as C and the

effective optical path length is expressed as L. Under the operation of signal modulation, the variation of emitting wavelength leads to the change of the absorption coefficient $\alpha(t)$, which is dependent on the emitting wavelength of DFB laser, expressed as Eq. (2). In Eq. (2), υ_0 is the central emitting light wave-number of the laser which is determined by the operation temperature described in chapter 3.2 in this paper with details, υ_g is the central absorption wave-number of gas molecular, α_0 is the light absorption coefficient at υ_0, γ is the half-width of the absorption peak at υ_0, and δ is light wavelength modulation coefficient.

$$\tau(\upsilon,t)=\frac{I(\upsilon)}{I_0(\upsilon)}=\exp[-\alpha(\upsilon,t)LC] \tag{1}$$

$$\alpha(t)=\frac{\alpha_0}{1+\left[\left(\upsilon_0+\delta u(t)-\upsilon_g\right)/\gamma\right]^2} \tag{2}$$

In this paper, the output wavelength of DFB laser has been modulated by a low frequency saw wave signal and a high frequency sine wave signal in order to satisfy the WMS detection theory. Therefore, the two signals above can be expressed as Eq. (3) and (4) respectively. In these equations, a and T_{saw} are the amplitude and the period of the saw signal, respectively. U_{saw} is the saw wave signal and time t is in the scope $0\le t\le T_{saw}$. In the sine wave signalU_{sin}, b and ω_{sin} are the amplitude and the angular frequency of the sine wave signal, respectively.

$$\mathrm{u_{saw}(t)\ =\ a\ +\ \frac{a}{T_{saw}}\ (t\ -\ T_{saw})} \tag{3}$$

$$u_{sin}(t)=b\sin(\omega_{sin}t) \tag{4}$$

In this way, two separated circuits have been developed to perform signal generation of Eq. (3) and (4). The circuits of DDS and DAC are shown in Fig. 1 where between the DSP and the additive laser driving circuit module in Fig. 1. The frequency of the saw wave signal and the sine wave signal is 10 Hz and 5 kHz respectively. Then, the emitting optical signal of the DFB laser can be shown in Eq. (5) where I_0 is the mean optical power at center wavelength and m is the modulation coefficient.

$$I(t)=I_0[1+mu_{ramp}(t)+mu_{sin}(t)] \tag{5}$$

Therefore, the final output of the DFB laser is the combination of the original wavelength, saw wave signal and the sine wave signal. The central wavelength of the laser can scan across the absorption line periodically according to the saw wave signal. And harmonic signals can be extracted by using the sine wave signal and further operations. The temperature controller and signal generation circuits related to the equations (2), (3) and (4) are shown in the photo

of the developed circuits as Fig. 5. The combined signal without absorption related to Eq. (5) is shown as the black waveform in Fig. 6.

3. Design details of key modules

3.1 System structure

The laser driver is demonstrated with experiments in this section. There are two major functions of the developed laser driver which are temperature control and current modulation. The schematic diagram of the DFB laser driver is shown in Fig. 1. As shown in the figure, a digital-signal-processor (DSP TMS320F28335) chip is applied to be the main controller in the system. It controls the developed Thermo Electrical Cooler (TEC) controller module to set and verify the laser's working temperature by using a 16-bit digital to analog converter (DAC). The TEC controller is ADN8831 that is a high precision monolithic TEC driver chip. The DSP also reads real-time laser temperature by using the analog to digital converter (ADC) circuit and the results can be shown on the LCD screen which is embedded in the front panel of the developed instrument. Meanwhile, according to WMS detection theory, a DDS circuit and a DAC circuit were developed to generate sine wave signal and saw wave signal respectively. The DFB laser is shown in Fig. 1. It is a 14-pin fiber coupled laser and the center wavelength is around 1563 nm which is suitable for sensing CO concentration in the near infrared region.

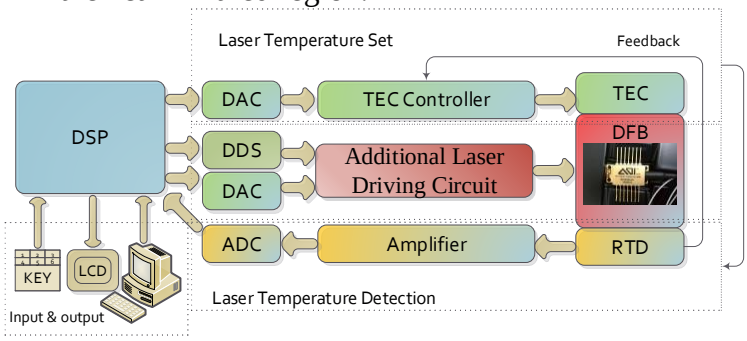

Fig. 1. Block diagram of the developed DFB laser driver.

3.2 Laser temperature controller

Laser temperature must be controlled effectively and accurately due to the fact that laser center wavelength is determined by laser temperature while driving current is fixed. According to the Peltier effect, the two sides of TEC will release and absorb heat respectively while current flow through. In this way, the laser temperature can be controlled by driving the TEC. The laser center wavelength can be controlled by varying laser temperature. According to the resistance-temperature table and experimental tests, the relationship between RTD value and

laser temperature can be determined as shown in Fig. 2 (a). Thus, the setting temperature can be performed by controlling the RTD value by the obtained fitting formula. In addition, further experiments were carried out and the relationship between the setting voltage and temperature was determined as shown in Fig. 2 (b). Therefore, the DFB laser temperature can be set and justified by using the DAC circuit to output corresponding voltage.

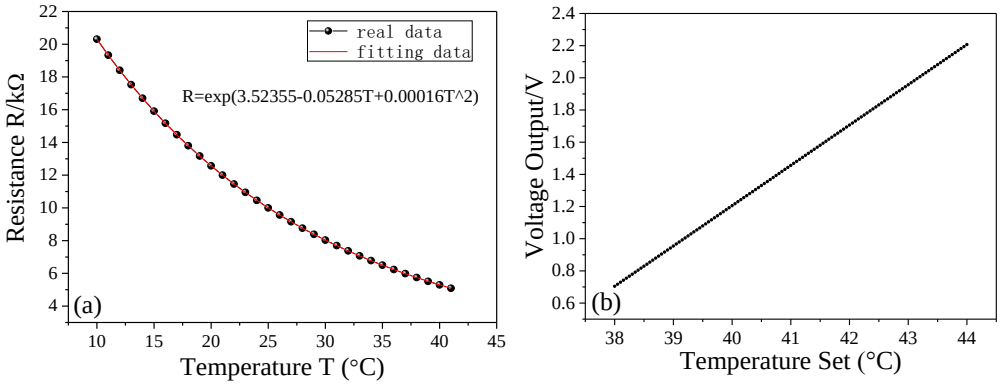

Fig. 2. Curve of RTH versus temperature (a) and the setting voltage versus temperature (b).

In Fig. 3, the laser temperature was measured by using the ADC circuit every 30 seconds during a total period of 24 hours. It can be seen that the laser fluctuation is maintained in the range ±0.02 ℃ around the setting value of 45.15 ℃. The fluctuation range is narrow enough to ensure the stability of the laser center wavelength. In addition, the response time test was performed by increasing and decreasing the temperature with a step of 1 ℃. The result is shown in Fig. 4 and it can be seen that the response time is less than 8 seconds and the overheating and overcooling range is within 3 ℃ without repeating thermal vibration. Therefore, experiment results suggesting good performance of the developed laser temperature controller.

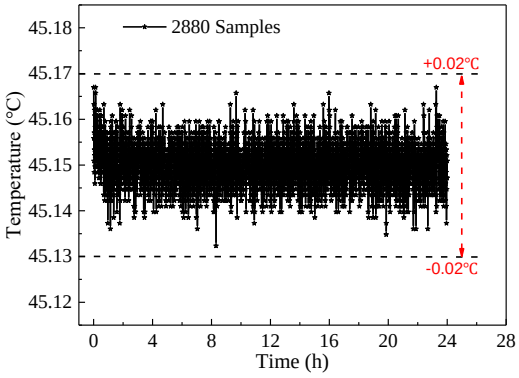

Fig. 3. Stability test of the laser temperature controller.

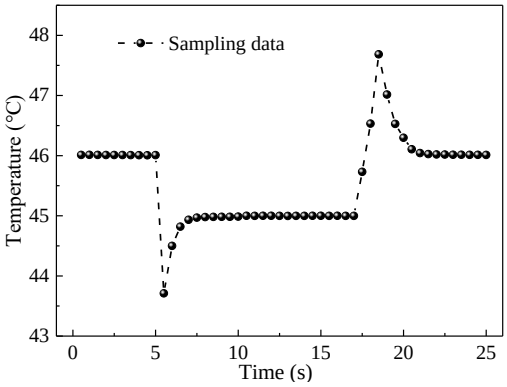

Fig. 4. Response time measurement of temperature modulation.

3.3 Laser current and signal controller

In WMS systems, the optical sources are generally simultaneously modulated by sine wave signal and saw wave signal for the extraction of harmonic signals. In this paper, the DFB laser is driven by the self-developed signal generator circuit. This circuit was designed and developed to generate a low frequency saw wave signal for swapping across the absorption line and a higher frequency sine wave signal as the modulating signal. The sine wave signal is generated by using a DDS chip, which is shown in Fig. 1. This DDS circuit can be controlled by DSP and is applied to generate sine signals at different frequency. The modulated signal must match with the backend of the system for harmonic extraction. In this system, 5 kHz sine wave signal is chosen as the modulating signal and a 10 Hz saw wave signal is chosen as the scan signal. The saw wave signal is generated by DSP along with a high accuracy DAC chip. The combination of the scan signal and the modulating signal can be applied to drive the DFB laser for the CO detection system based on the WMS technique. The developed board for laser temperature controlling and current driving is shown in Fig. 5.

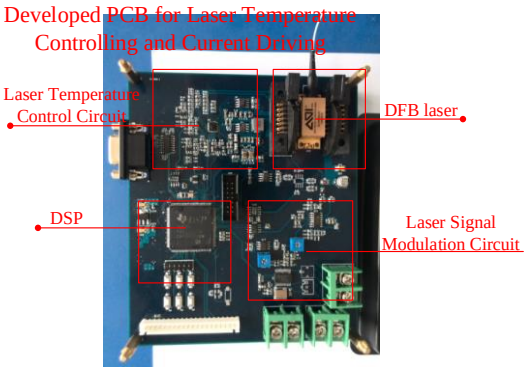

Fig. 5. Developed PCB for laser temperature controlling and current driving

The laser driving signals are crucial for gas concentration detection in WMS based systems. The spectrum must be stable and controllable effectively in order to meet the requirements of the sensing system. In our CO sensing system, the laser beam is divided into two power-equaled beams by using a fiber optic beam splitter (FOBS). One beam is linked to the gas cell as the absorption channel and the other beam is linked to optical attenuator (OA) as the reference channel. As mentioned above, the laser is driven by a 10 Hz saw wave signal and is modulated by a 5 kHz sine wave signal. Thus, the optical signals in the two channels are captured by two InGaAs photodiodes and are converted into electrical signals as shown in Fig. 6. The absorption signal, which is the red signal in Fig. 6, losses a certain part of power due to the phenomenon of CO gas absorption. Therefore, the value of the loss power can be obtained by the differential between the reference signal and the absorption signal. The loss power is proportion to CO concentration and effective optical path length. In this way, the CO concentration can be calculated and obtained.

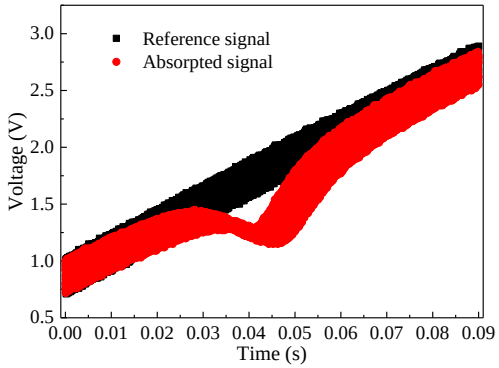

Fig. 6. Reference signal and detection signal under modulation of saw wave signal and sine wave signal.

4. Experiments

4.1 Experiment setup

During the CO sensing process, the DFB laser must be driven precisely and stable to meet the requirements of the experiments. The center wavelength must be controlled effectively by adjusting the laser temperature and driving current. Therefore, the relationship between spectrum and laser driving parameters are obtained by carrying out spectrum measurements. In order to evaluate the performance of the developed laser driver, spectrum measurements were performed by using a Fourier infrared spectrometer (Scientific, NICOLET 6700 FT-IR) which is shown in Fig. 7. The developed laser driver is integrated as a standalone instrument which is shown in Fig. 7. The FC/APC fiber port is embedded on the back panel of the instrument for linking optical fiber. After the

preparation of experiments setup, the relationship between spectrum and laser controlling parameters such as driving current and laser temperature were researched.

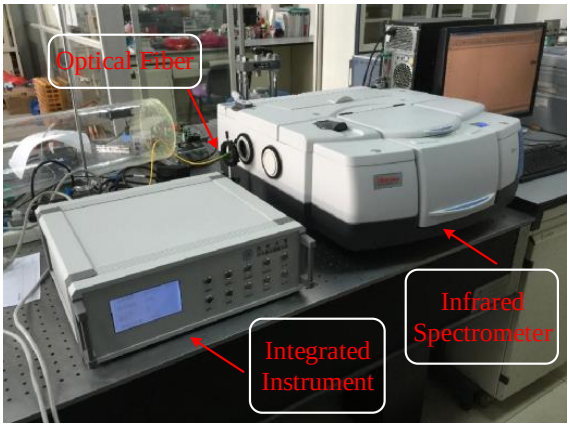

Fig. 7. Spectrum measurements by using the integrated DFB laser driver.

4.2 Spectroscopy measurement

The DFB laser driving current is set as 60 mA and its spectrum was measured while adjusting the laser temperature. The temperature was increased from 43 ℃ to 47 ℃ while the driving current was constant which is shown in Fig. 8. It can be seen that the center wavelength is shifted while the laser temperature is linearly tuned. The modulating coefficient can be obtained as 0.381cm-1/℃ by calculating the relationship between the variation of wavenumber and temperature. Meanwhile, it can be seen that the optical power is also changed while laser temperature varies.

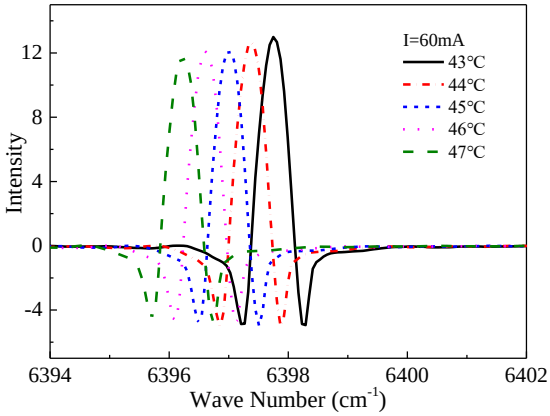

Fig. 8. Spectrum measurement with laser temperature variety from 43 ℃ to 47 ℃.

Then, spectrum was measured under the condition of changing current while laser temperature was fixed. As shown in Fig. 9, the center wavelength

shifts linearly while laser current is tuned linearly from 40 mA to 80 mA. The laser temperature is fixed as 45 ℃. Meanwhile, optical power is influenced by driving current obviously which is shown in Fig. 9. The optical power of the laser beam is proportional to the laser driving current and the coefficient can be obtained as about 0.027cm-1/mA by calculating. Results that is shown in Fig. 8 and 9 demonstrates the effectiveness and controllability of the self-developed laser driver.

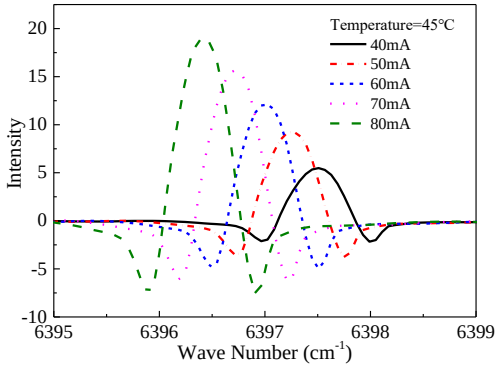

Fig. 9. Spectrum measurement with laser driving current variety from 40 mA to 80 mA.

4.3 Test of spectrum stability

The stability of laser wavelength is crucial for CO sensing experiments. Unstable wavelength causes huge error of the detection results. The stability of wavelength is affected by temperature fluctuation and noises in the electrical system. The center wavelength will shift, and the optical power will fluctuate ceaselessly if the driving conditions are not stable. Therefore, the test of spectrum stability was performed to evaluate the performance of the laser driver. In Fig. 10, the spectrum was measured every 10 minutes while the laser temperature and driving current were fixed at 45 ℃ and 60 mA respectively.

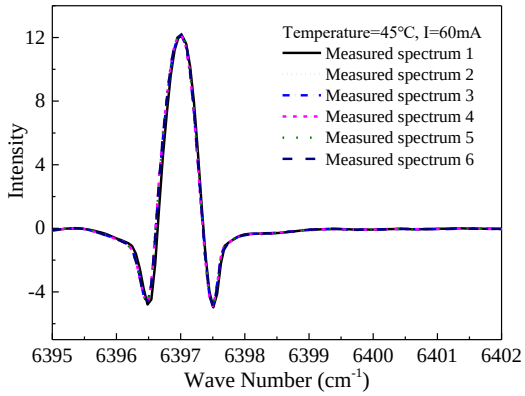

Fig. 10. Stability test of the laser center wavelength.

The resolution of the spectrum meter was set as 0.125 cm-1 during the experiments. It can be seen in Fig. 10, the measured spectrum show good repeatability for the six curves. The center wavelength is not shifted for each curve and the optical power remains the same value. This proves the stability of the developed laser driver.

4.4 Gas detection experiments

After the integration of the DFB driver, a CO detection system was established, and experiments were carried out to evaluate the performance of the laser driver. Standard concentrations of 10 CO samples were comparatively shown in Fig. 11 (a) with measured data. The relative error of each gas sample was calculated and are shown in Fig. 11 (b). Under the concentration of 10×104 ppm, the relative error becomes the maximum, which is about 3.8%. As shown in Fig. 11 (b), the absolute error increases while the concentration raises. Whereas, with the increasing of concentration, the relative error tends to be decreasing, and within the whole detection range, the relative detection error is within the range of −2.9%~3.8%. According to the gas detection experiments, the detecting error are remained in acceptable range. The effectiveness and stability of the developed laser driver were proved.

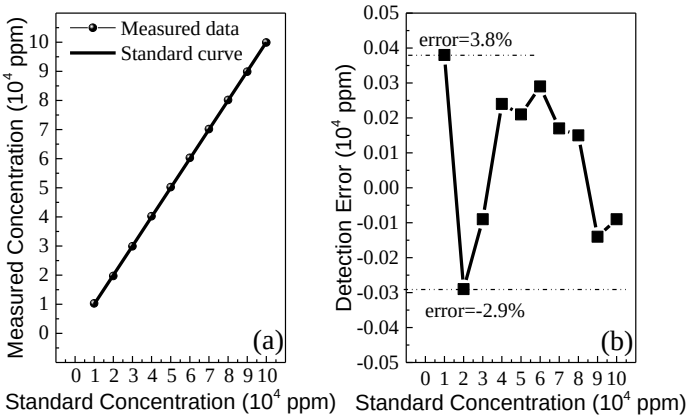

Fig. 11. (a) Measured concentrations as well as standard concentrations and (b) relative detection errors test

6. Conclusions

In order to satisfy the requirements of CO sensing system based on WMS technique, a distributed feedback laser driving instrument was self-developed and integrated as a standalone instrument. The center wavelength of the laser which is applied is around 1563.06 nm which is suitable for CO detection in the near infrared region. The developed instrument can be applied as the optical source of the CO sensing system and it replaces commercial instruments including laser temperature controller, current driver and signal generator. In this way, the total

cost of the CO sensing system can be limited into a more affordable region than using commercial instrument. Experiments were carried out to evaluate the performance of the integrated instrument. Firstly, stability and response time of laser temperature controller was tested. The fluctuation is in the region of ±0.02 ℃ and the response time was less than 8 seconds which proves good performance. Then, center wavelength under temperature & current control was measured to investigate the relationship. Spectroscopy measurements demonstrate good stability and linearity of the developed laser driver. Experimental results show that the developed and integrated instrument can be applied in WMS-based CO sensing system to achieve high stability, accuracy, lower cost and smaller size.

Acknowledgements

The authors wish to express their gratitude to the National Natural Science Foundation of China (No. 51672103), Jilin Jianzhu University, the National Key Technology R&D Program of the Ministry of Science and Technology of China, the Science and Technology Department of Jilin (20180201052SF, 20180201063SF), Province of China and the Education Department of Jilin Province of China (JJKH20180573KJ) for the generous support of this work.

REFERENCES

[1] *N. Sun, H. X. Liu, Z. Y. Yu, Z. N. Zheng, C. Y. Shao,* "The La0.6Sr0.4CoO3 perovskite catalyst for Li-O-2 battery", SOLID STATE IONICS, **vol. 268,** Dec. 2014, pp. 125-130.

[2] *S.B. Zhang, Y.C.Zhao, J.P.Yang, Y.Zhang, P.Sun, X.H.Yu, J.Y.Zhang and C.G.Zheng,* "Simultaneous NO and mercury removal over MnOx/TiO2 catalyst in different atmospheres", Fuel Processing Technology, **vol. 166,** Nov. 2017，pp. 282-290.

[3] *C. Gómez-Giménez, M.T. Izquierdo, M. de las Obras-Loscertales, L.F. de Diego, F. García-Labiano and J. Adánez,* "Mercury capture by a structured Au/C regenerable sorbent under oxycoal combustion representative and real conditions", Fuel, **vol. 207,** Nov. 2017，pp. 821-829.

[4] *Tarancon, A., Pena-Martinez, J., Marrero-Lopez, D., Morata, A., Ruiz-Morales, J. C., Nunez, P.,* "Stability, chemical compatibility and electrochemical performance of GdBaCo2O5+x layered perovskite as a cathode for intermediate temperature solid oxide fuel cells", SOLID STATE IONICS, **vol. 179,** no. 40, Dec. 2008, pp. 2372-2378.

[5] *Ashida, A.; Fujita, A; Shim, YG; Wakita, K; Nakahira, A,* "ZnO thin films epitaxially grown by electrochemical deposition method with constant current", THIN SOLID FILMS, **vol. 517**, no. 4, Dec. 2008, pp. 1461-1464.

[6] *E. Flores, J. Pizarro, F. Godoy, R. Segura, A. Gómez, N. Agurto and P. Sepúlveda,* "An electrochemical sensor for the determination of Cu(II) using a modified electrode with ferrocenyl crown ether compound by square wave anodic stripping voltammetry", Sensors and Actuators B: Chemical, **vol. 251,** Nov. 2017，pp. 433-439.

[7] *S.M. Hong, J.H. Jang,* "Transient Simulation of Semiconductor Devices Using a Deterministic Boltzmann Equation Solver", IEEE JOURNAL OF THE ELECTRON DEVICES SOCIETY, **vol.6,** no. 1, Dec. 2018, pp. 156-163.

[8] S*.A. Vladimirova, M.N. Rumyantseva, D.G. Filatova, A.S. Chizhov, N.O. Khmelevsky, E.A. Konstantinova, V.F. Kozlovsky, A.V. Marchevsky, O.M. Karakulina, J. Hadermann and A.M. Gaskov,* "Cobalt location in p-CoOx/n-SnO2 nanocomposites: Correlation with gas sensor performances", Journal of Alloys and Compounds, **vol. 721,** Oct. 2017, pp. 249-260.

[9] *F.X. Xin, J.J Guo, J.Y. Sun, J.L. Chao, F. Zhao and Z.S. Liu,* "Research on atmospheric CO2 remote sensing with open-path tunable diode laser absorption spectroscopy and comparison methods", Optical Engineering, **vol. 56,** Jun. 2017, pp. 066113.

[10] *Y.L. Wang; S.Y. Liu; Y. Feng, G.J. Wang; J.T. Zhu; L. Zhao,* "Infrared light absorption of silver film coated on the surface of femtosecond laser microstructured silicon in SF6", MATERIALS LETTERS, **vol. 63,** no. 30, Dec. 2009, pp. 2718-2720.

[11] *T. Nomoto, H. Onishi,* "Time-Domain Infrared-Visible-Visible Sum-Frequency Generation for Surface Vibrational Spectroscopy", JOURNAL OF PHYSICAL CHEMISTRY C, **vol. 113,** no. 52, Dec. 2009, pp. 21467 – 21470.

[12] *T. Kamimoto, Y. Deguchi, Y. Shisawa, Y. Kitauchi and Y. Eto,* "Development of fuel composition measurement technology using laser diagnostics", Applied Thermal Engineering, **vol. 102,** Jun. 2016, pp. 596-603.

[13] *J.S. Li, L.Z. Zhang, B.L. Yu,* "Site-selective nitrogen isotopic ratio measurement of nitrous oxide using a TE-cooled CW-RT-QCL based spectrometer", SPECTROCHIMICA ACTA PART A-MOLECULAR AND BIOMOLECULAR SPECTROSCOPY, **vol. 133,** Dec. 2014, pp. 489-494.

[14] *W. Wei, J. Chang, L.H. Cao, Y.H. Liu, X. Chen, C.H. Zhu and Z.H. Qin,* "Artificial absorption creation for more accurate tunable diode laser absorption spectroscopy measurement", Optics Communications, **vol. 399,** Sep. 2017, pp. 112-119.

[15] *Centeno R.; Marchenko D.; Mandon J.; Cristescu S.M.; Wulterkens G.; Harren F.J.M.,* "High power, widely tunable, mode-hop free, continuous wave external cavity quantum cascade laser for multi-species trace gas detection", APPLIED PHYSICS LETTERS, **vol. 105,** no. 26, Dec. 2014.

[16] *Z.F. Gong, K. C., Y.Y., X.l. Zhou, W. Peng and Q.X. Yu,* "High-sensitivity fiber-optic acoustic sensor for photoacoustic spectroscopy-based traces gas detection", Sensors and Actuators B: Chemical, **vol. 247,** May 2018, pp. 290-295.

[17] *F. Peng W.Jun Chang, Q.Wang, W.Wei and Z.G.Qin*, "TDLAS gas sensing system utilizing fiber reflector based round-trip structure: double absorption path-length, residual amplitude modulation removal", Sensors and Actuators A: Physics, **vol. 259,** Jun. 2017, pp. 152-159.

[18] *G.l. Zhang, J.g.Liu, Z.y Xu, Y.b. He and R.f.Kan,* "Characterization of temperature non‐uniformity over a premixed CH4–air flame based on line‐of‐sight TDLAS", Applied Physics B, **vol. 122,** no. 3, Jan. 2016.

[19] *A. Sepman, Y. Ögren, M. Gullberg and H. Wiinikka,* "Development of TDLAS sensor for diagnostics of CO, H2O and soot concentrations in reactor core of pilot‐scale gasifier", Applied Physics B, **vol. 122,** no. 2, Feb. 2016.